Carbon Nanotube Effect on Polyaniline Morphology in Water Dispersible Composites

Pablo Jiménez,* Pere Castell, Raquel Sainz, Alejandro Ansón, M. Teresa Martínez, Ana M. Benito, and Wolfgang K. Maser*

Instituto de Carboquímica (CSIC), Department of Nanotechnology, C/ Miguel Luesma Castán 4, 50018 Zaragoza, Spain

Received: September 21, 2009; Revised Manuscript Received: December 9, 2009

A straightforward, template-free chemical oxidative polymerization of aniline was used to prepare nanofibrillar polyaniline (nf-PANI) and a set of corresponding composites with multiwall carbon nanotubes (MWNTs). All the products showed remarkable water dispersibility since they are formed by hydrophilic particles of nanometric size. A comparative study performed on composites in a wide range of MWNT loadings has led to two main conclusions: on one hand, the presence of MWNTs affects neither the chemical structure nor the crystallinity of polyaniline. On the other hand, even small amounts of MWNTs have a significant effect on the morphology of polyaniline in composites. This effect is noticeable not only in electron microscopy images but also in the UV−vis absorbance of water dispersions and electrical conductivity behavior in the solid state. Competition between nucleation sites during polymerization is proposed as an explanation for these phenomena.

1. Introduction

One of the main trends in nanoscience research is focused on the precise control of the morphology in the production of nanostructures, such as the case of conducting polymers,[1] whose properties at nanometric scale are of special interest particularly in the field of organic electronics[2] (solar cells, light-emission diodes, field effect transistors, supercapacitors, actuators, chemical sensors, etc.). Among conducting polymers, polyaniline (PANI) stands out due to several reasons like its environmental stability, ease of synthesis, and versatile redox and chemical behavior.[3] The "classical" morphology of PANI is that of large, granular crystalline domains.[4] Nevertheless, in recent years an increasing collection of different nanostructures is being developed,[5] fibers, wires, tubes, spheres, flowers, ribbons, sheets, etc., using techniques ranging from hard- and soft-template to template-free strategies, either by chemical or electrochemical polymerization. Recent papers endeavored to explain the origin of these structures,[6] and despite some controversies, all point to the particular chemistry of the early stages of aniline oxidative polymerization. Another relevant line of research has comprised the combination of PANI with carbon nanotubes (CNTs) to yield nanocomposites with a combination or even an enhancement of properties from both components.[7] To improve the interaction and maximize the dispersion of both components, the favored preparative strategy has been the "in situ" polymerization of aniline in the presence of CNTs. Most examples of CNT−PANI composites show two characteristic bulk morphologies: the first one consists of PANI covered CNTs, in which the material is made of CNTs sheathed by a PANI layer of variable thickness,[8] and it is explained by the preferential growth of PANI chains on the nanotube surface. In the second one, CNTs are embedded in a PANI matrix, and here PANI displays a macrocrystalline morphology[9] that may be originated by subsequent growth and deposition of PANI on the initially formed "PANI covered CNTs" during polymerization, creating bigger aggregates. We recently reported a PANI−CNT material that showed a new kind of completely nanostructured morphology[10] since it was solely composed of nanofibrillar PANI (nf-PANI) and PANI covered CNTs. Its most remarkable property was the ease to prepare stable, surfactant-free water dispersions for composites up to 50 wt % in CNT content, which opens a novel approach for processing PANI−CNT composites.

In this work, we focus on the study of the modifications that different proportions of carbon nanotubes may induce in polyaniline and therefore in composite properties. A set of composites of PANI with different loadings of multiwalled arc-discharge carbon nanotubes (MWNTs) are prepared under identical synthetic conditions and then characterized. On the basis of our findings, these "CNT effects" can be divided into two groups: negligible effects on PANI structure and significant changes in PANI morphology. Given that our composites are solely made of discrete particles, both nf-PANI and PANI-covered MWNTs, morphological changes induced by CNTs are essentially alterations in the size and shape of those particles. Here we aim to explain how changes in morphology at the nanometric scale have great influence on some properties of the bulk material such as optical absorption in dispersions and electrical conductivity. It is important to remark that the mentioned effects induced by CNTs are particular for this kind of highly nanostructured composites, in which both components are nanostructured by themselves, and not applicable to other kinds of PANI−CNT composites reported in the literature, as will be discussed later. Our findings also enabled us to elucidate the special circumstances that lead to the formation of the nanostructured composite.

2. Experimental Section

2.1. Synthetic Procedure. Multiwalled carbon nanotubes were prepared by the arc-discharge method. A 25 V voltage and 60 A intensity current were employed to sublimate pure graphite rods under a helium atmosphere of 66 kPa. The inner core of the cathodic deposit was carefully collected and used without further purification; this material consisted mostly of

* Corresponding authors. E-mail: pablojm@icb.csic.es; wmaser@icb.csic.es.

10.1021/jp909093e
Published on Web 01/08/2010

straight MWNTs,[11] of micrometer lengths and diameters between 20 and 60 nm. nf-PANI and nf-PANI composites with MWNTs were prepared from distilled aniline (99.5%, Scharlau Chemie, Spain) and ammonium peroxydisulfate (APS, 98%, Sigma-Aldrich) as oxidant. Different percentages of MWNTs related to aniline were used in the preparation of composites, fom 1% (nf-PANI-1M) to 30% (nf-PANI-30M). In a typical reaction procedure, the appropriate amount of MWNTs was dispersed by sonication in 10 mL of aqueous HCl 1 M during 10 min, and nf-PANI was synthesized with no MWNTs as a reference material. Aniline (0.3 mL) was added and sonicated for 10 min. An APS (0.22 g) solution in 10 mL of HCl 1 M was added at once, and the reaction mixture was kept at 16−20 °C under sonication for 2 h. The mixture was then filtered, and the dark green solid was washed with HCl 1 M, then with ethanol and acetone. The product was dried under vacuum at room temperature for 24 h.

2.2. Characterization. Thermogravimetric analyses were performed on powder samples of the materials in a Setaram Setsys Evolution thermobalance at a heating rate of 3 °C/min under a constant air flow of 50 mL/min. Crystallinity of materials was studied by X-ray diffraction using a Bruker D8 ADVANCE diffractometer with the Cu Kα radiation at a 1.5418 Å wavelength. Aqueous dispersions of materials were prepared by sonication, in an ultrasonic bath during 5 min, of powder samples in HCl aqueous solutions at different concentrations. Ultraviolet−visible (UV−vis) absorption spectra were recorded on a Shimadzu U2401-PC spectrometer. Infrared absorption measurements were performed on powder samples pressed with KBr into pellets with a Bruker Vertex 70 spectrometer, and Raman spectra were recorded on powder samples with a Horiba Jovin-Yvon HRLAB HR 800 UV apparatus using an excitation laser with a wavelength of 532 nm. Scanning electron microscopy images were registered in a Hitachi S3400N microscope, and transmission electron microscopy was performed in a JEOL JSM-6400 after evaporation of a drop of diluted material dispersions onto a carbon-coated copper grid. For the conductivity measurements, pressed pellets of the materials were prepared with 5 wt. % of PVDF (poly(vynildifluoride)) as a binder, under a pressure of 5 tons for 2 min. A Keithley 4200-SCS semiconductor characterization system wired to tungsten tips was used to perform the four probe point conductivity measurements, and conductivities reported are average values from at least four measurements.

3. Resuts and Discussion

3.1. Synthesis of Composites. MWNT production in an arc-discharge reactor allowed the production of highly graphitized carbon nanotubes with a negligible amount of amorphous carbon and no trace of metal impurities. This was important since many transition metals usually found in CVD-CNTs (chemical vapor deposition produced nanotubes), such as iron, cobalt, or nickel, are able to form cations that can enhance the electron transfer processes and thus accelerate aniline oxidative polymerization.[12] This catalytic effect of transition metals could mask the effect of CNTs on PANI which is the object of this study. Two premises were pursued for the choice of the synthetic conditions: to be as simple as possible and to be applicable to all the ranges of MWNT compositions, which made the use of ultrasound irradiation compulsory to keep the different MWNT quantities in a similar state of suspension. As was described elsewhere, here aniline seemed to favor the aqueous dispersion of MWNTs, indicative of a preferential interaction of anilinium cations with the MWNT surface.[13] During the polymerization an acceleration of the reaction was clearly observed when nanotubes were present. Chemical oxidative polymerization of aniline in acidic media is known to have a slow first stage, called "induction period", when the initial reactants in solution remain colorless, followed by the emergence of a bluish hue corresponding to the first oxidized aniline oligomers.[14] Taking the time until the perception of this bluish hue as a reference for the duration of the induction period, the presence of MWNTs in the reaction media decreases the induction period from 4 min in nf-PANI to approximately 90 s in all composite polymerizations. Further observation of the subsequent polymerization stages was unfeasible owing to the inherent darkness of MWNTs in suspension.

TABLE 1: Composition of PANI−MWNT Materials

	MWNT (%)[a]	pol. yield[b]	MWNT (%)[c]	final T_{ox} (°C)[d]
nf-PANI	0	25%	0	-
nf-PANI-1 M	5.1	27%	4.5	820
nf-PANI-5 M	14.7	28%	13.6	846
nf-PANI-10 M	24.6	29%	23.5	872
nf-PANI-20 M	35.1	30%	34.3	887
nf-PANI-30 M	51.2	31%	47.1	900

[a] MWNT content = (initial MWNT weight/final composite weight) × 100. [b] Polymerization yield = (PANI weight in composites/theoretical weight of PANI for a complete conversion of aniline in PANI) × 100. [c] Values taken from MWNT weight loss in TGA. [d] Final temperature of the weight loss ascribed to MWNTs in composites.

In Table 1, calculated reaction yields are reported. These yields refer to aniline polymerization, assuming that during the reaction and purification procedure the total amount of MWNT is preserved. Under these reaction conditions, ammonium persulfate does not affect MWNT at all, proving that our arc-discharge nanotubes have a high stability toward oxidation as is also appreciated by TGA. A slight enhancement of the polymerization yield is observed for an increasing MWNT content. The increase of both polymerization rate and yield induced by MWNTs can be explained by a catalytic effect of the nanotube surface in the first stages of aniline oxidation, as will be discussed later.

3.2. Study of Polyaniline Structure in MWNT Composites. ***Thermogravimetry.*** Thermogravimetric analyses (TGA) of nf-PANI under air flow reveal the high stability of this kind of polyaniline. After desorption of moisture (until 120 °C), the main weight loss for PANI starts at about 300 °C and ends at 620 °C, for nf-PANI and all composites. In composites, oxidation of MWNTs starts always following the PANI decomposition, so its weight loss can be used reliably to determine the actual MWNT percentage. As can be seen in Table 1, nanotube weight percentages match reasonably well with the values estimated from the polymerization yield. Interestingly enough, the amount of nanotubes in the composites does not seem to affect the oxidation of PANI, but oxidation temperatures of nanotubes themselves are affected by the MWNT loading in composites. The MWNT decomposition starts at about 660 °C in all composites, but the corresponding temperature for the end of the oxidation rises gradually from 820 °C for nf-PANI-1 M to 900 °C for nf-PANI-30 M. These results indicate first that MWNTs do not modify the structure of PANI and second that nanotubes may be better dispersed in the less loaded composites since a worse segregation of MWNTs would cause higher MWNT oxidation temperatures.[15]

X-ray Diffraction (XRD). The XRD pattern of nf-PANI displays broad reflections at $2\theta \sim 25°$, 21°, 15°, and 9°, typical of HCl doped PANI synthesized by chemical polymerization

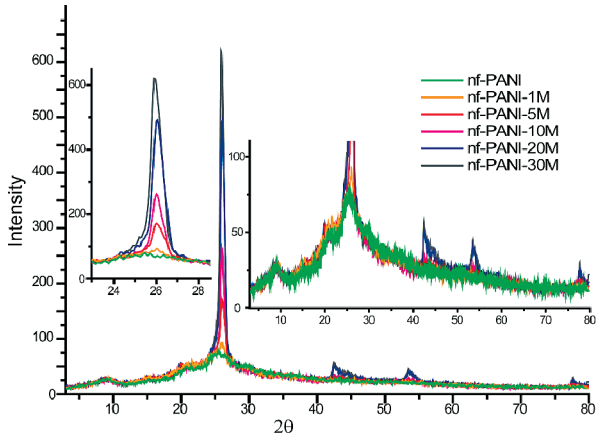

Figure 1. X-Ray diffractograms of materials. Insets show amplifications of MWNT main peak (left) and PANI diffraction pattern (right).

(Figure 1).[16] The more intense reflection at about 25° (corresponding to $d \sim 3.5$ Å) has been assigned to a regular spacing between phenyl rings of adjacent chains in a parallel orientation and is thus an indicator of PANI crystallinity. For MWNT composites, a much more intense reflection at $2\theta \sim 26°$ and smaller reflections at 43°, 54°, and 77° appear due to the highly graphitized arc-discharge multiwalled nanotubes.[17] The increase in the amount of nanotubes in the composite results in a greater relative intensity of the MWNT reflections, but no appreciable modification on the feature of PANI reflections is observed. This suggests that the presence of MWNT in composites does not introduce any additional order to PANI.

UV−visible Absorption Spectroscopy of Aqueous Dispersions. We took advantage of the high water dispersabilty of nf-PANI and composites and prepared homogeneous dispersions by sonication of the materials in aqueous solutions. Electronic absorption spectra of water dispersions of polyaniline and its composites are strongly pH dependent as was expected. "Emeraldine base" is the neutral, undoped, and unprotonated form of emeraldine, and "emeraldine salt" is considered to be the ionic, protonated, doped form. Nevertheless, every polyaniline chain possesses a large quantity of "protonable" nitrogen atoms, so there are plenty of intermediate species between the fully protonated and fully deprotonated forms that may display different absorption spectra. UV−vis absorption spectra of water dispersions at pH values of 3.7, 2.7, and 1.7 for nf-PANI and the composites at different MWNT loadings are presented (Figure 2). Three characteristic absorption bands appear, typical of the emeraldine salt state:[18] a band centered at about 360 nm, corresponding to a $\pi-\pi^*$ transition, a band at 430 nm assigned to a polaron$-\pi^*$ transition, and a broadband centered at around 860 nm, corresponding to a $\pi-$polaron transition. Relative intensity of the "polaron bands" (at 430 and 860 nm) related to the $\pi-\pi^*$ band clearly increases with acidity, indicative of an increased doping (i.e., a higher number of positively charged polarons in the chain) of the polymer due to the proton concentration in solution. In fact, at low pH (1.7) the $\pi-\pi^*$ band appears as a shoulder of the band centered at 430 nm, and at more basic pH (3.7) the 430 band appears as a shoulder of the 360 nm band. In agreement with the results of other spectroscopies presented here, the presence of MWNTs is not likely to modify either the chemical structure or the electronic states of polyaniline chains since neither appreciable shifts of the absorption bands nor changes in the relative intensity of bands are observed.

IR Spectroscopy. Synthesized nf-PANI and all its composites with MWNTs feature the same infrared absorptions. Since MWNTs do not exhibit specific absorption bands in the region between 400 and 4000 cm^{-1} of the spectra (only a featureless continuous IR absorption, as can be seen in its IR spectrum), the observed bands correspond to polyaniline absorptions. The IR spectra of the materials match well with that of HCl doped polyaniline,[19] and the most relevant bands are displayed in Table 2 with its corresponding assignments to vibrations or deformations. A strong "Fano effect" as asymmetrical shapes of the IR bands is also noticeable. This phenomenon is caused by overlapping of vibrational IR states with the electronic continuum of the polaron band in the doped PANI and is usually indicative of a highly conducting emeraldine salt state.[20] The lack of spectral differences between nf-PANI and its composites reflects that MWNTs do not induce changes on the chemical nature of polyaniline.

Raman Spectroscopy. nf-PANI, here in the emeraldine salt state, exhibits a quite intense Raman scattering, much stronger than arc-discharge MWNTs, so in our composites MWNT bands are masked by the PANI spectrum.[21] Hence, spectra of composites do not differ significantly from the spectrum of nf-PANI, as revealed in Figure 3. The most significant bands are listed in Table 2. The presence of MWNTs in composites is insinuated by a slight shift and deformation of the band at 1590 cm^{-1} toward lower wavenumbers that can be caused by the increasing proportional intensity of the G band of MWNTs[22] (the most intense band of arc-discharge MWNTs, localized around 1580 cm^{-1}). Raman spectroscopy, as well as our hitherto mentioned studies, suggests that no chemical or structural modifications take place in polyaniline owing to nanotube presence in composites.

3.3. Effect of MWNT on Composite Morphology. ***Scanning Electron Microscopy (SEM) and Transmission Electron Microscopy (TEM).*** SEM microscopy was performed on nf-PANI and its composites in emeraldine salt state, which was electrically conducting enough that gold covering of samples was unnecessary. SEM and TEM micrographs show that nf-

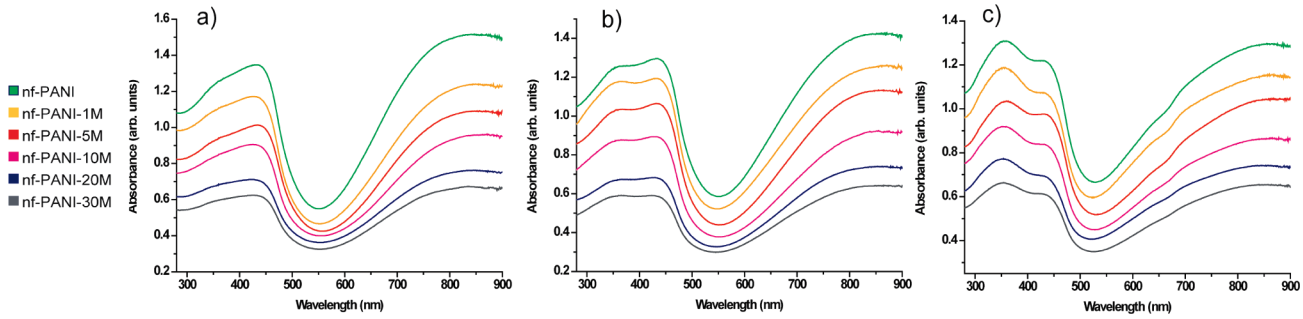

Figure 2. UV−vis absorption spectra of aqueous dispersions of materials at different pH: (a) at pH = 1.7; (b) at pH = 2.7; (c) at pH = 3.7.

TABLE 2: Main Bands Observed in IR and Raman Spectra and Their Assignments[a]

IR wavenumber (cm^{-1})	assignation	Raman shifts (cm^{-1})	assignation
505	C−H bending	420	C−N−C torsion
816	C−H bending	745	C−N−C bending
1140	−(N−H)+. bending	1166	C−H bending
1243	C−NH+. stretching	1346	C−NH+. stretching
1299	C−NH stretching	1497	C−C + C−N stretching
1481	C−C(Ben) stretching	1559	C−C (Qui) stretching
1559	C−C(Qui) stretching	1589	C−C (Ben) stretching

[a] Ben: benzenoid ring; Qui: quinoid ring.

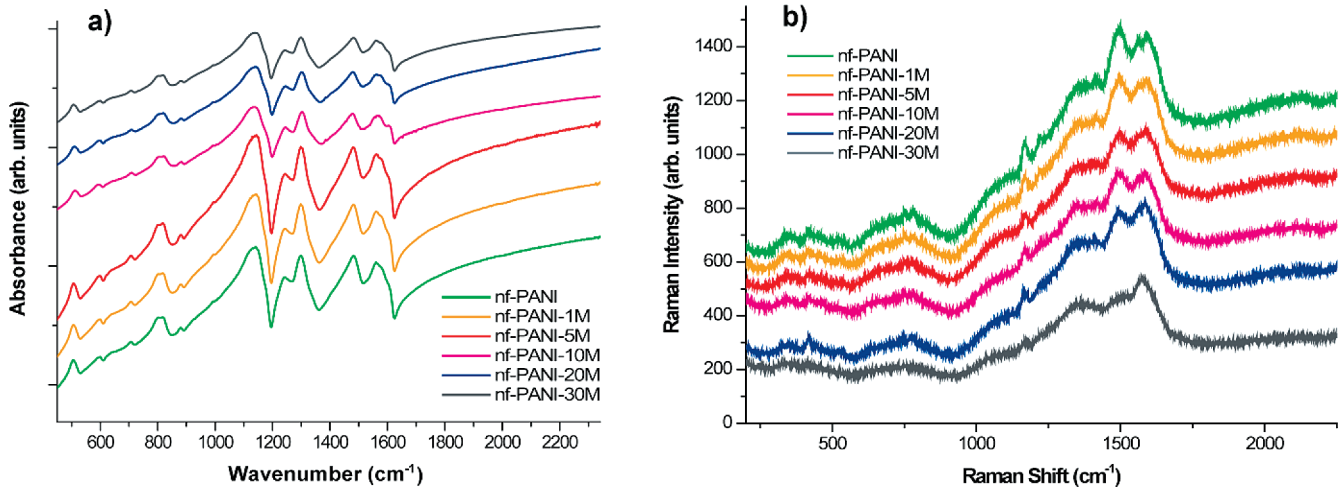

Figure 3. Infrared (a) and Raman (b) spectra of materials.

PANI is composed of nanometric elongated structures, their size being quite uniform: ca. 100 nm wide and 350 nm long. The origin of these structures may be the nanofibrils that are spontaneously formed by self-nucleation in the initial stages of polyaniline oxidative polymerization. In our case, PANI nanofibrils have developed into wider structures, but they have not coalesced into bigger aggregates, which explains the good water dispersibility of this material. These nanofibrillar structures are also present in all MWNT composite samples although smaller in size (see Figure 4). It seems that the presence of MWNTs, even at low concentrations, in the polymerization media leads to the formation of smaller nanofibrils. Microscopy images of composites indeed show a new kind of cylindrical, straight structure from which arc-discharge MWNTs are often visibly protruding. These structures are presumably formed through the nucleation and growth of polyaniline on the surface

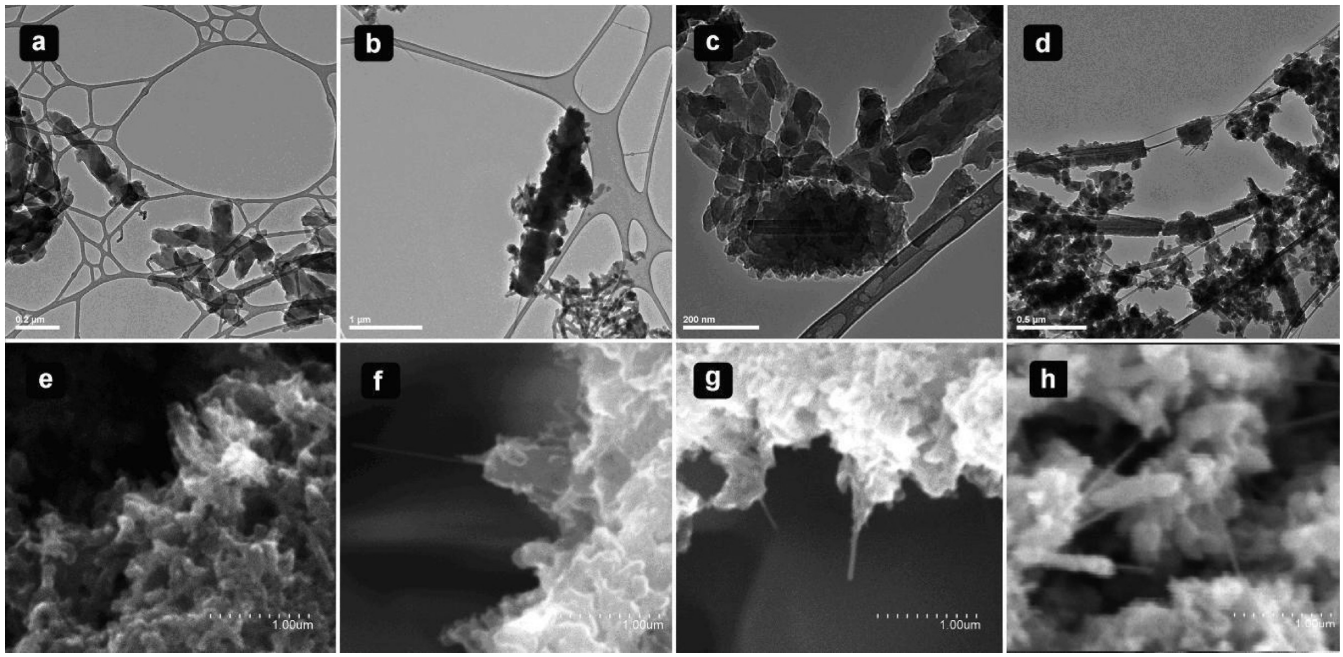

Figure 4. TEM (a−d) and SEM (e−h) images showing different structures visible in our materials corresponding to nf-PANI (a, e), nf-PANI-5 M (b, f), nf-PANI-10 M (c, g), and nf-PANI-30 M (d, h).

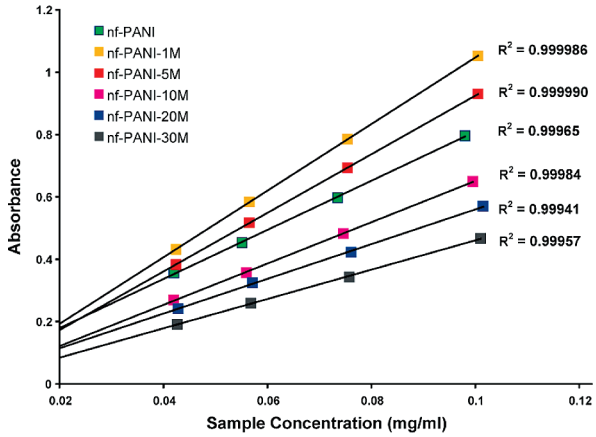

Figure 5. Absorbance vs concentration plot of aqueous dispersions of materials at pH = 2.7 at a wavelength of 431 nm. Values of standard deviations of least-squares linear fits are displayed.

of one or more MWNTs, and Figure 4c shows an unusually short MWNT completely covered by PANI grown on its surface. The length of this kind of PANI cylindrical covering is variable, but normally it does not reach the nanotube lengths; i.e., nanotubes are not completely covered by PANI. The diameter of these cylinders also seems to decrease with the nanotube content, and the diameter is about 400 nm in nf-PANI-5 M and 180 nm in nf-PANI-30 M. This phenomenon can be explained by an enhanced availability of nucleation surface, provided by the MWNTs on which the existing aniline monomers will have to be distributed and polymerized.

UV−vis Absorption Studies at Different Concentrations. As has been mentioned, the most remarkable property of these composites is their high water dispersibility, which allowed us to perform optical absorption studies on homogeneous dispersions. To compare the UV−vis absorption properties of aqueous dispersions of composites at different loadings of nanotubes, a more detailed study at various concentrations was performed. We found that a pH value of 2.7 was optimal for the stability of water dispersions of nf-PANI and its composites, in agreement with previous studies on nanofibrillar polyaniline dispersions.[23] A clear linear dependence of absorbance with concentration was observed for nf-PANI and all the composites, and as can be seen in Figure 5, this suggests that our dispersions are composed of individual, well-dispersed particles in that range of concentrations. Here the presence of MWNTs in composites does seem to affect the absorptivity of the samples. Our arc-discharge MWNTs have less absorptivity in the visible region than PANI in emeraldine salt state, and as a result, some composite dispersions (10 M, 20 M, and 30 M) have less absorptivity than the nf-PANI sample, which makes sense taking into account the lower amount of PANI present in those samples. However, the less loaded composite samples (1 M and 5 M) unexpectedly showed higher absorptivities. This effect can be explained in terms of variation of the particle size caused by nanotube presence in the synthesis of composites. In small particle homogeneous dispersions, absorptivity (this term includes absorption and light scattering) is strongly dependent on the size of particles in suspension.[24] In general, for the same mass concentration and in the same conditions, a substance made of smaller particles "absorbs" more light. As was shown in SEM images of composites, PANI can exist in two kinds of structures: the smaller, free nf-PANI nanofibrillar particles and the larger cylinders wrapping MWNTs, whose size decreases with nanotube content. If the dispersion of our products is envisaged as a suspension of noninteracting, separated particles of different

TABLE 3: Values for Parameters Refined Employing Equation 1[a]

	z_p[b]	x_m	extinction coefficients[b]	
nf-PANI	1	0	ε'_m (λ = 363 nm)	1.389
nf-PANI-1 M	0.764	0.042	ε'_m (λ = 431 nm)	0.987
nf-PANI-5 M	0.786	0.148	ε'_m (λ = 869 nm)	0.782
nf-PANI-10 M	1.013	0.244	ε'_p (λ = 363 nm)	8.095
nf-PANI-20 M	1.009	0.346	ε'_p (λ = 431 nm)	8.236
nf-PANI-30 M	1.067	0.470	ε'_p (λ = 869 nm)	8.986

[a] Values obtained through iterative least squares fit of experimental data to formula (1), x_m = weight fraction of MWNTs in materials, z_p = size factor, ε'_m = corrected extinction coefficient for MWNTs, ε'_p = corrected extinction coefficient for PANI. [b] Parameters defined in the Supporting Information.

sizes, Beer−Lambert law can be appropriate to model the absorption behavior of our samples. Classic Beer−Lambert expression relates absorbance with concentration of absorbing species but does not include particle size as a variable parameter (see details in Supporting Information). In fact, this expression is derived from the more general one that relates absorbance with the concentration of light absorbing particles and their effective cross-section area.[24] We can assume that effective cross-section area of our particles, for each wavelength and in the same conditions, is directly proportional to their geometric cross section area. Following the equation development depicted in the Supporting Information, we can express the absorbance due to polyaniline in terms of concentration of PANI, a modified extinction coefficient ε'_p, and a monodimensional size factor designed as z_p. For ideal elongated cylindrical objects, this size factor is directly proportional to their diameter and independent of its length.

$$A(\lambda) = C\cdot\left(\frac{x_p\cdot\varepsilon'_p(\lambda)}{z_p} + x_m\cdot\varepsilon'_m(\lambda)\right) \qquad (1)$$

Experimental parameters introduced in eq 1 are the total absorbance of the composite dispersions A, weight concentration C, and weight fractions of PANI x_p and MWNTs x_m (from TGA measurements, see Table 1). This equation enabled us, through a least-squares fit of experimental data, to estimate values of parameters such as the corrected extinction coefficients for MWNTs ε'_m, the size factor z_p, and even weight fractions for each composite composition, as can be seen in Table 3. It is relevant to emphasize that the calculations are consistent enough to refine values for MWNT extinction coefficients and weight compositions that are in agreement with our experimental data. The size factor $z_p = 1$ has been arbitrarily assigned to nf-PANI to compare average sizes of PANI particles in composites. This model provided a good fit of weight fractions of MWNTs and PANI that matched with values obtained by TGA. The size factor gives an idea of the average diameters or thicknesses of polyaniline structures, that is, PANI nanofibers and cylinders. In 1 and 5 M samples, the size factor of PANI particles is lower than for nf-PANI, which can be explained by the relative lower size of the particles in those materials, as was seen in SEM images (Figure 4). The relative amount of larger PANI cylinders increases with the nanotube loading, causing an increase in the size factor. However, this effect is compensated with the mentioned reduction of the average diameter of cylinders, resulting in a size factor that only reaches a value of 1.067 for the 30 M sample.

Electrical Conductivity. Figure 6 shows the conductivity values at room temperature measured on pressed pellets of nf-

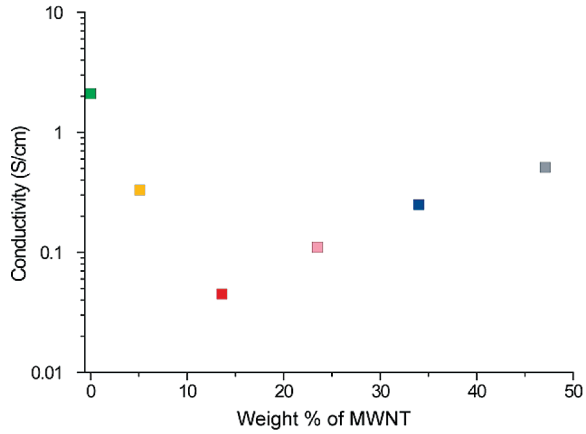

Figure 6. Four-point conductivity values for pressed pellets.

PANI and different compositions of PANI−MWNT composites. In these composites, both components (PANI in emeraldine salt state and arc-discharge MWNTs) are electrically conducting materials and have room temperature conductivity values of the same order of magnitude. The highest conductivity is achieved for nf-PANI pellets, and surprisingly, conductivity decreases for the less loaded samples and then increases with nanotube content. As we observed neither spectroscopic nor structural changes in polyaniline, we can presume that the intrinsic conductivity of polyaniline does not change. These changes in measured bulk conductivity should be then caused by changes in morphology, this being another example of a clear nanoscale morphology effect in macroscopic properties, characteristic of highly nanostructured materials. Long et al. have reported that bulk conductivity of nanostructured conducting PANI is largely determined by the contact resistance between particles and generally is not representative of the actual conductivity of polyaniline.[25] For example, they estimated that resistance contact between PANI nanotubes ascended to 500 kΩ, about 16 times the resistance measured across an individual tube. Both components, PANI and MWNTs, are quite conducting materials, and therefore bulk conductivity measured in pellets is determined by the density of resistive contacts between individual particles. A smaller particle size results in a higher number of resistive contacts between particles per unit volume, thus lowering bulk conductivity. Observed values of conductivity point to that phenomenon since the presence of MWNTs during polymerization reduces the average size of free nf-PANI that outnumbers the rest of the particles. The subsequent increase in conductivity of the more loaded samples (10 M, 20 M, and 30 M) can be assigned to an enlargement of the average PANI particle size (as was pointed out by UV−vis absorbance of dispersions), to the increase of the relative amount of CNT−CNT contacts (whose resistance would be lower than inter-PANI contacts), or possibly to a combination of both effects.

Origin of Nanostructure during Polymerization. The spontaneous generation of nanofibers in the initial stages of PANI in polymerization with chemical oxidants in aqueous acidic media is a general phenomenon.[26] If the subsequent growth of PANI on nanofibers is suppressed or controlled, a nanostructured material can be obtained instead of the classical macrocrystalline PANI. The simplest reported method is that of rapid mixing of reactants, which is template-free and proceeds in aqueous media.[27] In syntheses of nf-PANI, the rapid mixing of reactants (aniline and oxidant) causes the formation of a high number of nucleation sites in suspension, and the growth of PANI on those sites is controlled by the available concentration of reactants in solution. Recent papers deal with the origin of the nucleation species on which aniline oligomers consecutively add to form the chain of polyaniline. The most probable structure is that of aniline oligomers with phenazine structure that are hydrophobic in nature.[6a] This hydrophobicity would cause the segregation of these species in an aqueous media that may be the origin of nanofibers in suspension. It also explains the formation of thin PANI layers on practically any available surface, even at the air−water interface, that may be caused by the arrangement of monolayers of these hydrophobic oligomers.[28]

In the polymerization process of our composites, MWNTs are hydrophobic species partially dispersed in water thanks to ultrasonic irradiation, and any accessible surface of MWNTs would be preferentially covered by the hydrophobic oligomers formed in the initial stages of oxidation. These surfaces can facilitate the contact between those reactants and the amphiphyllic anilinium cations in the aqueous reaction media, causing some catalytic effect on the polymerization as was suggested by experimental observations. Nanotube surfaces hence become nucleation sites that compete with the suspended aggregates that generate the free nanofibers, also increasing the total amount of nucleation sites. Due to the straight shape of our well graphitized nanotubes, PANI grown on MWNT surfaces has a cylindrical shape. The fact that nanotubes are not completely covered by PANI indicates that MWNTs themselves are not completely dispersed at the initial stages of polymerization (that is, there is a certain area of MWNTs that is in close contact with other MWNT surfaces and thus not accessible to reactants in the reaction media) and that further dispersion of MWNTs may be favored by its partial hydrophilic PANI covering. The presence of MWNTs causes the initial adsorption of aniline and probably accelerates the production rate of the mentioned hydrophobic aniline oligomers. This catalytic effect in the initial stage of polymerization is supported by the mentioned observation of an earlier appearance of the blue color due to oligomers. Then again, we observed a slight but not substantial increase in the polymerization yield with the introduction of nanotubes,[10] which means that polymerization of aniline reaches its completion within the reaction time. Therefore, two effects may arise from MWNT presence: first the catalytic effect of MWNTs causes an increase in the number of hydrophobic aggregates in suspension, in this case assisted by ultrasonic irradiation. Second, there is an increase in the number of nucleation sites (both aggregates in suspension and effective surface of MWNTs) which would compete for the existing aniline monomers during the growth of PANI chains. This effect reduces the amount of PANI polymerized on each nucleation site, i.e., decreases the size of PANI individual nanostructures (nanofibrils and cylinders) at the end of the reaction. The observed scenario then would match these premises, the lower size of nf-PANI nanofibrils and the decrease in the thickness of PANI-MWNT cylinders with an increasing amount of MWNTs.

The lack of structural changes in PANI, which is perceived regardless of the amount of MWNTs, suggests that the PANI polymerization mechanism does not change and also indicates the lack of a strong interaction between PANI and MWNTs. Some papers report on the modification of spectroscopic properties of PANI in CNT composites that is justified by a $\pi-\pi$ stacking between the nanotube walls and polymer chains parallel to them.[8c,9b,c] In the case of our composites, we can presume that this parallel stacking would be hindered by aniline nucleates attached to the nanotube surface as well as by the subsequent growth of PANI chains perpendicular to that surface.[29]

4. Conclusions

A set of nanostructured composites of PANI with different MWNT concentrations were prepared to evaluate and compare its properties. The effect of MWNTs was manifest on the nanostructure of the material; in general, the presence of MWNTs in composites reduced the size of free-standing PANI covering the tubes. Hence, MWNTs had a clear effect on some properties dependent on morphology such as optical absorptivity of dispersions and bulk conductivity. Conversely, spectroscopic properties and crystallinity of PANI are not affected by nanotube loading. In summary, modifications in the nanostructure of composites that appear as nanotubes provide a large hydrophobic surface for the adsorption of oligomeric species that initiate the growth of PANI, whose structure and features are practically identical to pure nanofibrillar PANI. These experimental results provide an example of how the comprehension and control of morphology formation is of great importance in the development of nanostructured self-assembled composites.

Acknowledgment. Funding from the Spanish Ministry of Science and Innovation (MICINN) and the European Regional Development Fund (ERDF) under projects MAT2006-13167-C02-02 and MAT20007-66927-C02-01, as well as from the Government of Aragon (DGA) under Consolidated Group Program (DGA-T66 CNN) and Project DGA-PI086/08 is gratefully acknowledged. P.J. gratefully acknowledges 'Fundación Ramón Areces' for his Ph.D. grant and DGA/CAI (Programa Europa XXI) for their financial support.

Supporting Information Available: Derivation of eq 1 and description of the procedure employed to calculate the parameters listed in Table 3. This material is available free of charge via the Internet at http://pubs.acs.org.

References and Notes

(1) (a) Gangopadhyay, R.; De, A. *Chem. Mater.* **2000**, *12*, 608. (b) Jang, J. *Adv. Polym. Sci.* **2006**, *199*, 189. (c) Aleshin, A. N. *Adv. Mater.* **2006**, *18*, 17.

(2) Brabec, C.; Sariciftci, N.; Hummelen, J. *Adv. Funct. Mater.* **2001**, *11*, 15. (b) Wanekaya, A.; Chen, W.; Myung, N.; Mulchandani, A *Electroanalysis* **2006**, *18*, 533. (c) Bäcklund, T.; Sandberg, H.; österbacka, R.; Stubb, H.; Mäkelä, T.; Jussila, S. *Synth. Met.* **2005**, *148*, 87. (d) Ho, P. K. H.; Kim, J. I-S.; Burroughes, J. H.; Becker, H.; Li, S. Y. F.; Brown, T. M.; Cacialli, F.; Friend, R. H. *Nature* **2000**, *404*, 481. (e) Rudge, A.; Davey, J.; Raistrick, I.; Gottesfeld, S.; Ferraris, J. P. *J. Power Sources* **1994**, *47*, 89. (f) Mirfakhrai, T.; Madden, J. D. W.; Baughman, R. H. *Mater. Today* **2007**, *10*, 30. (g) Hatchett, D. W.; Josowicz, M. *Chem. Rev.* **2008**, *108*, 746. (h) Ling, Q.-D.; Liaw, D.-J.; Teo, E.-Y.; Zhu, C.; Chan, D. S-H.; Kang, E.-T.; Neoh, K.-G. *Polymer* **2007**, *48*, 5182.

(3) MacDiarmid, A. G. *Angew. Chem., Int. Ed.* **2001**, *40*, 2581.

(4) Stejskal, J.; Riede, A.; Hlavatá, D.; Prokeš, J.; Helmstedt, M.; Holler, P. *Synth. Met.* **1998**, *96*, 55.

(5) (a) Zhang, D.; Wang, Y. *Mater. Sci. Eng., B* **2006**, *134*, 9. (b) Huang, J.; Kaner, R. B. *Angew. Chem., Int. Ed.* **2004**, *43*, 5817. (c) Huang, J.; Kaner, R. B. *J. Am. Chem. Soc.* **2004**, *126*, 851. (d) Anilkumar, P.; Jayakannan, M. *Macromolecules* **2008**, *41*, 7706. (e) Sajanlal, P. R.; Sreeprasad, T. S.; Nair, A. S.; Pradeep, T. *Langmuir* **2008**, *24*, 4607. (f) Janosevic, A.; Ciric-Marjanovic, G.; Marjanovic, B.; Holler, P.; Trchova, M.; Stejskal, J. *Nanotechnology* **2008**, *19*, 135606. (g) Stejskal, J.; Sapurina, I.; Trchova, M.; Konyushenko, E. *Macromolecules* **2008**, *41*, 3530. (h) Chiou, N.-R.; Lee, L. J.; Epstein, A. J. *Chem. Mater.* **2007**, *19*, 3589. (i) Han, S.; Briseno, A. L.; Shi, X.; Mah, D. A.; Zhou, F. *J. Phys. Chem. B* **2002**, *106*, 6465. (j) Anilkumar, P.; Jayakannan, M. *Langmuir* **2008**, *24*, 9754. (k) Amarnath, C. A.; Kim, J.; Kim, K.; Choi, J.; Sohn, D. *Polymer* **2008**, *49*, 432.

(6) (a) Sapurina, I.; Stejskal, J. *Polym. Int.* **2008**, *57*, 1295. (b) Zhang, X; Kolla, H. S.; Wang, X.; Raja, K.; Manohar, S. K. *Adv. Funct. Mater.* **2006**, *16*, 1145. (c) Zhong, W.; Wang, Y.; Yan, Y.; Sun, Y.; Deng, J.; Yang, W. *J. Phys. Chem. B* **2007**, *111*, 3918. (d) Surwade, S.; Manohar, N.; Manohar, S. K. *Macromolecules* **2009**, *42*, 1792.

(7) (a) Sainz, R.; Benito, A. M.; Martinez, M. T.; Galindo, J. F.; Sotres, J.; Baro, A. M.; Corraze, B.; Chauvet, O.; Maser, W. K. *Adv. Mater.* **2005**, *17*, 278. (b) Wu, T. M.; Lin, Y. W.; Liao, C. S. *Carbon* **2005**, *43*, 734. (c) Yu, Y. J.; Che, B.; Si, Z. H.; Li, L.; Chen, W.; Xue, G. *Synth. Met.* **2005**, *150*, 271. (d) Yan, X. B.; Han, Z. J.; Yang, Y.; Tay, B. K. *J. Phys. Chem. C* **2007**, *111*, 4125. (e) Maser, W. K.; Jiménez, P.; Payne, N. O.; Shepherd, R. L.; Castell, P.; in het Panhuis, M.; Benito, A. M. *J. Nanosci. Nanotechnol.* **2009**, *9*, 6157.

(8) (a) Konyushenko, E. N.; Stejskal, J.; Trchova, M.; Hradil, J.; Kovarova, J.; Prokes, J.; Cieslar, M.; Hwang, J. Y.; Chen, K. H.; Sapurina, I. *Polymer* **2006**, *47*, 5715. (b) Li, L.; Qin, Z.-Y.; Liang, X.; Fan, Q.-Q.; Lu, Y.-Q.; Wu, W.-H.; Zhu, M.-F. *J. Phys. Chem. C* **2009**, *113*, 5502. (c) Feng, W.; Bai, X. D.; Lian, Y. Q.; Liang, J.; Wang, X. G.; Yoshino, K. *Carbon* **2003**, *41*, 1551–1557.

(9) (a) Deng, J.; Ding, X.; Zhang, W.; Peng, Y.; Wang, J.; Long, X.; Li, P.; Chan, A. S. C. *Eur. Polym. J.* **2002**, *38*, 2497. (b) Ginic-Markovic, M.; Matisons, J. G.; Cervini, R.; Simon, G. P.; Fredericks, P. M. *Chem. Mater.* **2006**, *18*, 6258–6265. (c) Sainz, R.; Benito, A. M.; Martinez, M. T.; Galindo, J. F.; Sotres, J.; Baro, A. M.; Corraze, B.; Chauvet, O.; Dalton, A. B.; Baughman, R. H.; Maser, W. K. *Nanotechnology* **2005**, *16*, 150.

(10) Jiménez, P.; Maser, W. K.; Castell, P.; Martínez, M. T.; Benito, A. M. *Macromol. Rapid Commun.* **2009**, *30*, 418.

(11) Benito, A. M.; Maser, W. K.; Martínez, M. T. *Int. J. Nanotechnol.* **2005**, *2*, 71.

(12) (a) Stejskal, J.; Gilbert, R. G. *Pure Appl. Chem.* **2002**, *74*, 857. (b) Stejskal, J.; Kratochvil, P.; Spirkova, M. *Polymer* **1995**, *36*, 4135.

(13) Philip, B.; Xie, J.; Abraham, J. K.; Varadan, V. K. *Polym. Bull.* **2005**, *53*, 127.

(14) Wei, Y.; Tang, X.; Sun, Y.; Focke, W. *J. Polym. Sci., Part A* **1989**, *27*, 2385.

(15) Wei, H. F.; Hsiue, G. H.; Liu, C. Y. *Compos. Sci. Technol.* **2007**, *67*, 1018.

(16) Pouget, J. P.; Jozefowicz, M. E.; Epstein, A. J.; Tang, X.; MacDiarmid, A. G. *Macromolecules* **1991**, *24*, 779.

(17) Saito, Y.; Yoshikawa, T.; Bandow, S.; Tomita, M.; Hayashi, T. *Phys. Rev. B* **1993**, *48*, 1907.

(18) Xia, Y.; Wiesinger, J. M.; MacDiarmid, A. G.; Epstein, A. J. *Chem. Mater.* **1995**, *7*, 443.

(19) (a) Ping, Z. *J. Chem. Soc., Faraday Trans.* **1996**, *92*, 3063. (b) Quillard, S.; Louarn, G.; Lefrant, S.; MacDiarmid, A. G. *Phys. Rev. B* **1994**, *50*, 12496. (c) Quillard, S.; Louarn, G.; Buisson, J. P.; Boyer, M.; Lapkowski, M.; Pron, A. *Synth. Met.* **1997**, *84*, 805.

(20) Tigelaar, D. M.; Lee, W.; Bates, K. A.; Saprigin, A.; Prigodin, V. N.; Cao, X.; Nafie, L. A.; Platz, M. S.; Epstein, A. J. *Chem. Mater.* **2002**, *14*, 1430.

(21) (a) Quillard, S.; Berrada, K.; Louarn, G.; Lefrant, S. *New J. Chem.* **1995**, *19*, 365. (b) Berrada, K.; Quillard, S.; Louarn, G.; Lefrant, S. *Synth. Met.* **1995**, *69*, 201. (c) Cochet, M.; Louarn, G.; Quillard, S.; Buisson, J. P.; Lefrant, S. *J. Raman Spectrosc.* **2000**, *31*, 1041. (d) Lindfors, T.; Ivaska, A. *J. Electroanal. Chem.* **2005**, *580*, 320.

(22) Filho, A. G. S.; Jorio, A.; Samsonidze, G. G.; Dresselhaus, G.; Saito, R.; Dresselhaus, M. S. *Nanotechnology* **2003**, *14*, 1130.

(23) Li, D.; Kaner, R. B. *Chem. Commun.* **2005**, 3286.

(24) Gregory, J. *Particles in water*; CRC Press: Boca Raton, FL, 2005.

(25) Long, Y.; Zhang, L.; Ma, Y.; Chen, Z.; Wang, N.; Zhang, Z.; Wan, M. *Macromol. Rapid Commun.* **2003**, *24*, 938.

(26) Huang, J.; Kaner, R. B. *Chem. Commun.* **2006**, 367.

(27) Li, D.; Kaner, R. B. *J. Am. Chem. Soc.* **2006**, *128*, 968.

(28) Stejskal, J.; Sapurina, I. *Pure Appl. Chem.* **2005**, *77*, 815.

(29) (a) Sapurina, I.; Osadchev, A. Yu.; Volchek, B. Z.; Trchova, M.; Riede, A.; Stejskal, J. *Synth. Met.* **2002**, *129*, 29. (b) Orlov, A. V.; Kiseleva, S. G.; Karpacheva, G. P. *Polym. Sci. - Ser. A* **2008**, *50*, 1021.

JP909093E